

International Conference on Martensitic Transformations, ICOMAT-2014

## Microstructural characterization and transformation behavior of porous Ni<sub>50.8</sub>Ti<sub>49.2</sub>

X. Yao<sup>a</sup>, S. Cao<sup>b</sup>, X.P. Zhang<sup>b</sup>, D. Schryvers<sup>a,\*</sup>

<sup>a</sup>EMAT, University of Antwerp, Groenenborgerlaan 171, B-2020 Antwerp, Belgium

<sup>b</sup>School of Materials Science and Engineering, South China University of Technology, Guangzhou 510640, China

---

### Abstract

Porous Ni<sub>50.8</sub>Ti<sub>49.2</sub> bulk material was prepared by powder metallurgy sintering. Solid solution and aging treatments were applied to improve the phase homogeneity and phase transformation behavior. Scanning and transmission electron microscopy, aided by energy dispersive X-ray analysis, were used to study the microstructure and chemical phase content of the alloys. In-situ cooling was carried out to observe the phase transformation behavior. As-received material contains dispersed Ni<sub>2</sub>Ti<sub>4</sub>O particles while Ni<sub>4</sub>Ti<sub>3</sub> precipitates appear after aging. Close to pore edges, the latter have a preferential orientation due to the induced stress fields in the matrix.

© 2015 The Authors. Published by Elsevier Ltd. This is an open access article under the CC BY-NC-ND license (<http://creativecommons.org/licenses/by-nc-nd/4.0/>).

Selection and Peer-review under responsibility of the chairs of the International Conference on Martensitic Transformations 2014.

*Keywords:* Porous NiTi; Precipitate; R-phase; Strain field

---

### 1. Introduction

Shape memory alloys (SMA) are one of the early examples of smart materials and are at present used in many commercial applications. Among these alloys, the Ni-Ti binary alloy attracted much attention not only because it is one of the early discovered SMAs and well developed in recent decades but also because of its unusual properties aside the shape memory and superelasticity effects, such as good biocompatibility and good corrosion resistance. After decades of investigations on dense SMAs, porous forms of Ni-Ti were recently introduced. While retaining the

---

\* Corresponding author. Tel.: 0032 32653247 ; fax: 0032 32653318.

E-mail address: [nick.schryvers@uantwerpen.be](mailto:nick.schryvers@uantwerpen.be)

excellent properties of dense alloys, porous Ni-Ti has more potential applications especially in biomedical technology. The pore structure of the alloy permits ingrowth of body tissue into the foreign implant yielding a stronger fixation at the implant-bone interface than for dense alloys. Moreover, the Young's modulus and strength of the implant can be controlled by changing the porosity of the alloy to approach the mechanical properties of the bone while the similarity of implant-bone stiffness prevents stress-shielding behavior and osteoporosis diseases. [1]

Fabrication methods of porous Ni-Ti alloys have been widely studied and reported, including conventional sintering (CS) [2], self-propagating high-temperature synthesis (SHS) [3,4], spark plasma sintering (SPS) [5] and traditional hot isostatic pressing (HIP) processes [6]. All of these fabrication methods yield specific characteristics on pore features and mechanical properties: pore size and shape are hard to control via the CS method; SHS produces samples that have a high porosity and small pore size while the SPS method produces samples with low porosity and small pore size. The HIP method can fabricate samples with a relatively low porosity and it is rather easy to control the pore features, but this method requires high pressure and high temperature during the process which makes the fabrication not very cost-effective.

All methods mentioned are based on powder metallurgy controlled by a diffusion transformation, and normally introduce secondary particles such as  $\text{NiTi}_2$  and  $\text{Ni}_3\text{Ti}$  in the alloy matrix during syntheses. The present study on the microstructure of these porous alloys will help to gain a systematic understanding, which will enable a control in properties, especially for the shape memory effect and its applications in biomedical and engineering devices.

## 2. Experimental

Porous  $\text{Ni}_{50.8}\text{Ti}_{49.2}$  was prepared from pure nickel (99.9%, 50  $\mu\text{m}$ ) and titanium (99.9%, 50  $\mu\text{m}$ ) powders (mean particle size of 50 and 61  $\mu\text{m}$ , respectively) mixed together and blended by a V-blender for 24h and subsequently cold compacted into so-called green samples with a geometry of  $16 \times 10$  (diameter  $\times$  height,  $\text{mm}^2$ ) using a hydraulic presser. In the present work no space holders were used. The stress applied on the sample was 100 MPa. The sintering process was carried out in a quartz tube furnace under the protection of flowing argon (99.99% purity). The temperature was increased in steps from room temperature till 1000  $^\circ\text{C}$ , where the sample was held for 3 h followed by water quenching. Different cuts from this as-received material were then treated in different ways, or by a follow-up solid solution treatment at 1000  $^\circ\text{C}$  for 10 h and/or by an aging treatment at 500  $^\circ\text{C}$  for 6 h, both under vacuum and followed by water quenching.

Surfaces for Scanning Electron Microscopy (SEM) investigations were produced by gentle grinding with an abrasive of silicon oxide while a dual-beam Focused Ion Beam (FIB) - SEM was used to produce Transmission Electron Microscopy (TEM) samples, allowing the preparation of samples from different locations: region with secondary phase particles, matrix without secondary phase particles, and regions next to a pore. TEM was performed using FEI CM20 and Tecnai G2 instruments, both equipped with an Energy Dispersive X-ray (EDX) detector. In-situ TEM liquid nitrogen cooling experiments has been performed on all but the as-received sample to investigate the phase transformation behaviour.

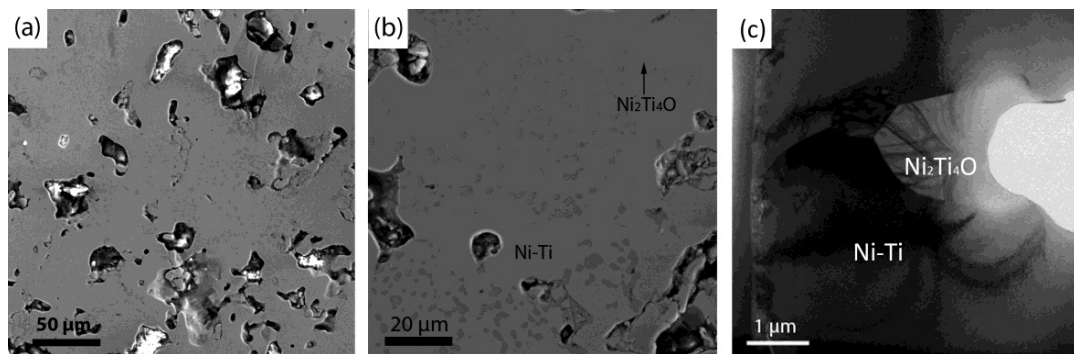


Fig. 1. (a) (b) SEM images on the surface of the bulk porous NiTi, (c) TEM bright field image with second phase.

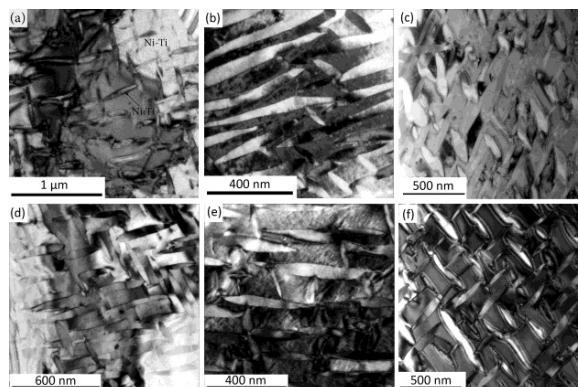


Fig. 2. Bright field images of  $\text{Ni}_4\text{Ti}_3$  precipitates from an aged sample: (a) matrix area with  $\text{Ni}_2\text{Ti}_4\text{O}$ , (b) close to a pore and (c) pure matrix ((a) and (c) are away from any pore); same site selection (d, e, f) from a sample aged after solid solution.

### 3. Results

#### 3.1 Phase distribution of porous $\text{Ni}_{50.8}\text{Ti}_{49.2}$

Figure 1 shows room temperature SEM images (a & b) at different magnifications and representative for all samples (here taken from the aged sample). Typical randomly shaped pores with sizes from  $5\ \mu\text{m}$  till  $60\ \mu\text{m}$  in the area of observation can be seen (the bright contrast inside the pores are  $\text{SiO}_2$  remnants from the surface polishing). In the enlargement in Fig. 1b the secondary electron contrast reveals a matrix containing regions with micron-scale secondary phase particles. TEM EDX measures have shown that the matrix is Ni-rich (on average 56 at.% Ni – 44 at.% Ti) while the secondary phase is  $\text{Ni}_2\text{Ti}_4\text{O}$ , explaining the Ni enrichment of the matrix. Fig. 1c shows such a secondary phase particle by bright field (BF) TEM in a FIB sample obtained from the respective region.

#### 3.2 Effect of pores on $\text{Ni}_4\text{Ti}_3$ precipitation

The pores of the samples were formed during the sintering procedure. Since some space exists between the Ni and Ti powder particles prior to any thermal treatment, pores are formed before other precipitates such as  $\text{NiTi}_2$  and  $\text{Ni}_4\text{Ti}_3$  will appear. Fig. 2 is a series of BF images of  $\text{Ni}_4\text{Ti}_3$  precipitates from an aged sample: (a) matrix area with  $\text{Ni}_2\text{Ti}_4\text{O}$ , (b) close to a pore and (c) pure matrix ((a) and (c) are away from any pore); same site selection (d, e, f) from a sample aged after solid solution. Close to the pores one variant of the  $\text{Ni}_4\text{Ti}_3$  precipitates is seen to be prevalent due to the stress field surrounding the pore and preferring one variant family extending along the tensile strain direction perpendicular to the edge of the pore.

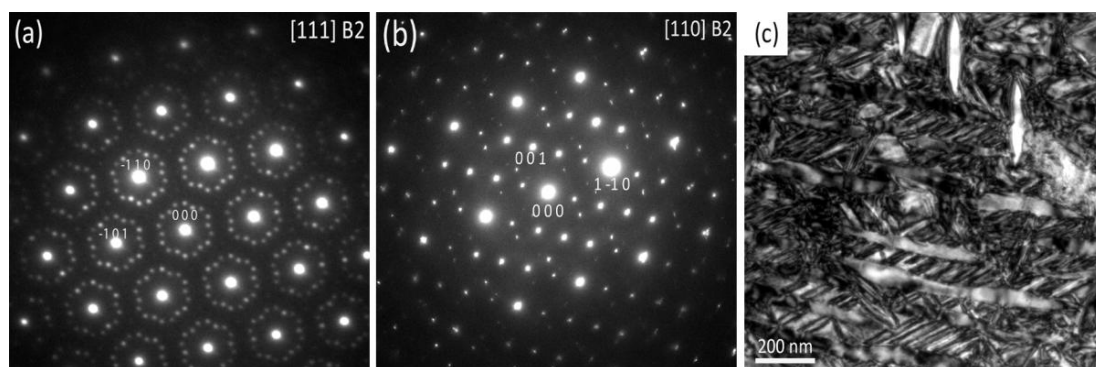


Fig. 3. (a) and (b) diffraction patterns of the sample aged after solid solution and taken at a temperature of  $-175^\circ\text{C}$ . (c) is the bright field image revealing  $\text{Ni}_4\text{Ti}_3$  precipitates and twinned R-phase.

### 3.3 Phase transformation behavior

Figure 3 illustrates the phase transformation behavior upon in-situ TEM cooling to liquid Nitrogen temperature of an aged sample close to a pore. Fig. 3a and 3b are  $[111]_{B2}$  matrix and  $[110]_{B2}$  matrix diffraction pattern respectively, revealing the coexistence of  $Ni_4Ti_3$  and R-phase at  $-175\text{ }^\circ\text{C}$ . The BF image in Fig. 3c reveals twinned R-phase grown between two elongated  $Ni_4Ti_3$  precipitates. Regions with smaller and randomly distributed  $Ni_4Ti_3$  precipitates did not show such well-developed R-phase microstructures.

## 4. Discussion

The present porous  $Ni_{50.8}Ti_{49.2}$  samples prepared from nickel and titanium powders without space holders reveal random shaped pores between 5 and 60  $\mu\text{m}$ . Regions with pure B2 phase matrix as well as dual-phase B2 +  $Ni_2Ti_4O$  areas exist in between the pores in the as-received material (with final treatment of 3h at  $1000\text{ }^\circ\text{C}$ ) as well as in the solid solution material (extra 10h treatment at  $1000\text{ }^\circ\text{C}$ ). The existence of micro-scaled  $Ni_2Ti_4O$  particles even after the annealing processes thus indicates that the cold compression at 100MPa of micro-sized Ni and Ti particles produces a far from homogeneous material with Ti-rich and Ni-rich regions. Aging at  $500\text{ }^\circ\text{C}$  produces the expected  $Ni_4Ti_3$  precipitates in every sample, which is consistent with the TTT diagram for Ni-Ti [7]. For the latter, no difference between clean B2 matrix regions or B2 +  $Ni_2Ti_4O$  regions could be found so far, but strain fields accompanying the pores induce preferential growth of selected  $Ni_4Ti_3$  orientation variants close to the pore surfaces.

The  $Ni_4Ti_3$  precipitates have the well-known lenticular shape with an average diameter of around 400 nm for those away from the pores. For the precipitates next to the pores, most appeared around only 100 nm in diameter while one family reaches up to 600 nm in diameter, which are expected values for aging at  $500\text{ }^\circ\text{C}$  according to the work by T. Tadaki et al. [8]

## 5. Conclusion

The main room temperature phase in porous  $Ni_{50.8}Ti_{49.2}$  alloys is the B2 austenite with dispersed  $Ni_2Ti_4O$  particles while  $Ni_4Ti_3$  precipitates appear after aging. This is quite similar to the dense alloy indicating that pores as such have no direct influence on the phase formation. Still, pores cause strain in surrounding regions, which influences the nucleation and growth of the  $Ni_4Ti_3$  precipitates. Variants of the latter have a preferential orientation along the tensile strain direction, which is perpendicular to the edges of the pores. Such a preferential growth also affects the appearance and distribution of the R-phase and possibly the martensite in the porous alloy. Twinned R-phase grows between two elongated  $Ni_4Ti_3$  precipitates and forms a parallel twinned structure consisting of two variants. Elongated  $Ni_4Ti_3$  precipitates close to a pore thus promote the nucleation and growth of the R-phase.

## Acknowledgements

The author gratefully acknowledges the Chinese Scholarship Council (CSC) for providing a scholarship and the Key Project of the Natural Science Foundation of Guangdong Province under grant No. S2013020012805.

## References

- [1] C. Greiner, S.M. Oppenheimer, D.C. Dunand, *Acta Bio.* 1 (2005) 705–716.
- [2] S.M. Green, D.M. Grant, N.R. Kelly, *Powder Metall.* 40 (1997) 43–47.
- [3] M. Ottaguchi, Y. Kaieda, N. Oguro, *J. Japan Inst. Metals.* 54 (1990) 214–223.
- [4] B.Y. Li, L.J. Rong, V.E. Gjunter, *J. Mater. Res.* 15 (2000) 10–13.
- [5] Y. Zhao, M. Taya, Y.S. Kang, A. Kawasaki, *Acta Mater.* 53 (2005) 337–343.
- [6] D.C. Lagoudas, E.L. Vandygriff, *J. Intel. Mater. Syst. Struct.* 13 (2002) 837–850.
- [7] M. Nishida, C.M. Wayman, T. Honma, *Metall. Trans.* 17A (1986) 1505–1515.
- [8] T. Tadaki, Y. Nakata, K. Shimizu, K. Otsuka, *Trans. JIM.* 27 (1986) 731–740.